Profilin Interacts with the Gly-Pro-Pro-Pro-Pro-Pro Sequences of Vasodilator-Stimulated Phosphoprotein (VASP): Implications for Actin-Based *Listeria* Motility

Fan Kang,[‡] Roney O. Laine,[‡] Michael R. Bubb,[‡,§] Frederick S. Southwick,[‡,§] and Daniel L. Purich*[,‡]

Departments of Biochemistry & Molecular Biology and Medicine, University of Florida College of Medicine, Health Science Center, Gainesville, Florida 32610-0245

Received January 13, 1997; Revised Manuscript Received April 16, 1997[⊗]

ABSTRACT: Intracellular actin-based motility of *Listeria monocytogenes* requires protein−protein interactions involving two different proline-rich sequences: first, the tightly bound bacterial surface protein ActA uses its multiple oligoproline registers [consensus sequence = FE(D)FPPPPTD(E)E(D)] to tether vasodilator-stimulated phosphoprotein (VASP) to the bacterial surface; and second, VASP then deploys its own multiple GPPPPP (or GP_5) registers to localize the actin−regulatory protein profilin to promote actin polymerization. We now report that fluorescence titration showed that $GP_5GP_5GP_5$ peptide binds to profilin (K_D of 84 μM), and the peptide weakly inhibits exchange of actin-bound nucleotide in the absence or presence of profilin. Microinjection of synthetic GPPPPP triplet into *Listeria*-infected PtK2 cells promptly arrested motility at an intracellular concentration of 10 μM. This inhibition was completely neutralized when equimolar concentrations of profilin and $GP_5GP_5GP_5$ were simultaneously microinjected. Fluorescence studies with [His-133-Ser]-profilin, a site-directed mutant previously shown to be defective in binding poly-L-proline [Bjorkegren, C., Rozycki, M., Schutt, C. E., Lindberg, U., & Karlsson, R. (1993) *FEBS Lett. 333*, 123−126], exhibits little or no evidence of saturable $GP_5GP_5GP_5$ binding. When an equimolar concentration of this [His-133-Ser]-profilin mutant was co-injected with $GP_5GP_5GP_5$, the peptide's inhibitory action remained completely unaffected, indicating that $GP_5GP_5GP_5$ binding to wild-type profilin represents a key step in actin-based pathogen motility. We also present a model that shows how the focal binding of VASP with its GPPPPP registers can greatly increase the local concentration of profilin and/or profilin−actin−ATP complex at the bacteria/rocket-tail interface.

The gram-positive bacillus *Listeria monocytogenes* offers an excellent model system for studying actin-based motility within nonmuscle cells. After phagocytosis by the host cell, this pathogen rapidly escapes the phagolysosome and enters the cytoplasm where it proliferates and then induces actin filament assembly (Tilney & Portnoy, 1989; Dabiri et al., 1990; Southwick & Purich, 1995; 1996). Bacterial locomotion results from the rapid elongation of actin filament rocket tail structures, and the assembly of new filaments provides the force for intracellular movement (Dabiri et al., 1990; Sanger et al., 1992). New actin monomers add to the plus-ends of actin filaments at the bacterial/rocket tail junction, while monomers are released from the minus-ends at the distal end of the tail (Dabiri et al., 1990; Theriot et al., 1992). Transposon mutation experiments indicate that the surface protein ActA is required for *Listeria*-induced actin assembly (Kocks et al., 1992). ActA protein contains tandem oligoproline repeats, and microinjection of synthetic CFEFPPPPTDE, itself corresponding to second sequence repeat, blocks *Listeria* motility at 30−100 nM intracellular concentrations (Southwick & Purich, 1994). When these experiments were first performed, profilin was the only actin regulatory protein known to interact with poly-L-proline (Tanaka & Shibata, 1985). Accordingly, we proposed a model wherein the introduction of the synthetic analogue FEFPPPPTDE competitively blocked profilin binding to ActA, thereby arresting *Listeria*'s actin-based motility (Southwick & Purich, 1994). A shortcoming of this one-step model was that the concentrations of the ActA peptide analogue needed to block bacterial motility are substoichiometric by a factor of about 50−300 relative to the profilin concentration (10−60 μM) in nonmuscle cells. The recent discovery that the host cell component vasodilator-stimulated phosphoprotein (or VASP)[1] is concentrated at the rear of migrating *Listeria* cast new light on these apparently contradictory findings (Chakraborty et al., 1995). VASP is a tetrameric protein with each of its subunits containing four GPPPPP sequences thought to be involved in profilin binding. A two-step binding process, involving VASP interaction at ActA's proline-rich sequences and profilin interaction at VASP's GPPPPP sequences, appears to be essential for bacterial motility. Beyond its involvement in *Listeria* locomotion, VASP is localized at focal contacts and membrane ruffles, sites of active actin filament assembly in uninfected cells (Reinhard et al., 1995), suggesting that VASP may be part of a host cell regulatory pathway for stimulating actin assembly during normal migration and stress fiber formation.

* Address all correspondence to this author at Department of Biochemistry & Molecular Biology, University of Florida College of Medicine, Box 100245, Health Science Center, 1600 Archer Avenue, Gainesville, FL 32610-0245. Tel: (352) 392-1546. FAX: (352) 392-2953. E-mail: dlpurich@biochem.med.ufl.edu.

‡ Department of Biochemistry & Molecular Biology.

§ Department of Medicine.

⊗ Abstract published in *Advance ACS Abstracts,* June 15, 1997.

[1] Abbreviations: VASP, vasodilator-stimulated phosphoprotein; $GP_5GP_5GP_5$, GPPPPPGPPPPPGPPPPP sequence repeat of VASP; ϵ-ATP, 1,N^6-etheno-ATP; DTT, dithiothreitol; WASP, Wiskott−Aldrich syndome protein; Ena, the gene protein of the *Drosophila* gene *enabled.*

S0006-2960(97)00065-2 CCC: $14.00

Profilin's binding to GPPPPP sequences in VASP thus appears to be a critical step in actin-based *Listeria* motility. From studies with the octadecapeptide $GP_5GP_5GP_5$, we now report (a) that this synthetic peptide binds to profilin in vitro; (b) that $GP_5GP_5GP_5$ weakly inhibits profilin-promoted exchange of actin-bound nucleotides with added nucleotide; (c) that $GP_5GP_5GP_5$ inhibits intracellular *Listeria* motility; (d) that this inhibition is completely neutralized by co-injection of equimolar wild-type profilin; (e) that the [His-133-Ser] mutant of profilin fails to bind $GP_5GP_5GP_5$, and (f) that this mutant cannot block $GP_5GP_5GP_5$ inhibition of intracellular *Listeria* locomotion. Our findings are consistent with models in which the two different oligoproline-containing proteins ActA and VASP work in concert to localize profilin at the rear of moving bacteria (Southwick & Purich, 1996; Zeile et al., 1996). This two-tiered binding process occurs within a discrete layer on the bacterium, and the local concentration of GPPPPP registers may well exceed 1 mM, thereby assuring the availability of profilin and/or profilin−actin to promote actin-based motility of this pathogen.

MATERIALS AND METHODS

Proteins and Peptides. Recombinant human profilin was expressed in *Escherichia coli* [strain BL21(DE3) pLysS] using the modified pET vector, pMW172 (Way et al., 1990; Federov et al., 1994). Purification of the profilin was as previously described (Federov et al., 1994; Machesky et al., 1994) with some modification. Briefly, packed cells from a 1 L culture were resuspended in 40 mL of buffer containing 50 mM Tris-HCl, 1 mM DTT, 1 mM EDTA (pH 8.0) and lysed by sonication, and homogenate centrifuged at 100000*g* for 1 h at 4 °C. After 25 mM KCl was added to the final expression supernatant, this material was passed through a 15 cm × 20 mm DEAE-5wp column (TOSOHAAS, Philadelphia) preincubated with the same buffer. The flow-through was concentrated to approximately 10 mg/mL, using Centriprep-3 concentrators (Amicon, Inc., Beverly, MA), and loaded onto a HiLoad 16/60 Superdex 200 gel filtration column (Pharmacia, Inc., Piscataway, NJ) preequilibrated with 50 mM Tris-HCl, 50 mM NaCl, 1 mM DTT, 1 mM EDTA, pH 8.0, and 2.5 mL fractions were collected. Profilin fractions were evaluated by SDS−PAGE, and spectrophotometry was used to evaluate yields. The profilin concentration was measured by UV absorbance at 280 nm using an extinction coefficient of 0.015 OD μM^{-1} cm^{-1} (Tseng et al., 1984). To prepare the mutant profilin, nucleotide primers containing appropriate restriction sites were introduced into the coding sequence of the human platelet profilin mutant by PCR and the modified DNA was ligated into the pMW172 vector used in the wild-type profilin expression described above. The His-133-Ser mutant does not bind poly-L-proline (Bjorkegren et al., 1993), and the bacterially expressed mutant and wild-type profilins were purified by identical techniques.

$GP_5GP_5GP_5$ peptide was synthesized by the automated Merrifield method, and purity of the HPLC-purified peptide was confirmed by acid hydrolysis and determination of amino acid composition. Commercial poly-L-proline (Sigma Chemical Company, St. Louis) had an average molecular weight of 5600, corresponding to about 57 residues.

Actin was purified from outdated human platelets according to Weber et al. (1992) with minor modification. Briefly, platelet acetone powder was prepared from washed platelets (15 units). To extract actin, acetone powder was stirred with 15 mL of actin extraction buffer [2 mM Tris-HCl, 0.2 mM ATP, 0.6 mM β-mercaptoethanol, 0.5 mM $CaCl_2$ (pH 8.0)] at 2 °C for 0.5 h. After centrifugation for 2 h at 100000*g* at 2 °C, actin supernatant was collected and concentrated to 5 mL using a Centriprep-30 concentrator (Amicon, Inc., Beverly, MA). The concentrated actin sample was then loaded onto a HiLoad 16/60 Superdex 200 gel filtration column (Pharmacia) preequilibrated with actin extraction buffer. The actin-enriched fractions from the column were collected, combined, and concentrated to 2.2 mL. One cycle of polymerization and depolymerization of actin was carried out as described elsewhere (Weber et al., 1992). Depolymerization of actin was made by dialysis in the cold against G-buffer [2 mM Tris-HCl, 0.5 mM DTT, 0.2 mM ATP, 0.1 mM $CaCl_2$, 0.2 mM sodium azide (pH 7.5)] for 3 days with three changes of the buffer. The yield of actin was 5.6 mg and the purity was higher than 98% as determined by SDS−PAGE. The actin concentration was measured by UV absorbance at 290 nm using an extinction coefficient of 0.026 OD μM^{-1} cm^{-1} (Tseng et al., 1984).

Fluorescence Measurements. Binding of $GP_5GP_5GP_5$ peptide to profilin was monitored by the change of tryptophan fluorescence using a photon counting spectrofluorometer (Photon Technology International, model A1010). The excitation wavelength was set to 295 nm, and the emission spectra from 310 to 400 nm were recorded. The titration of profilin with the peptide was performed by the addition of aliquots of a concentrated peptide at 20 °C. The concentration of profilin was 5 μM, and the buffer was 20 mM Hepes, pH 7.4, containing 1 mM DTT in the presence or absence of 150 mM KCl.

Nucleotide Exchange Kinetics. Exchange of actin-bound ATP with free 1,N^6-etheno-ATP (or ϵATP) was measured by fluorescence (Goldschmidt-Clermont et al., 1991), using an excitation wavelength of 340 nm and emission wavelength of 415 nm. The 1 mL assay mixture (pH 7.2) contained 0.6 μM Ca-ATP-G-actin, 2 mM Tris, 2 μM $CaCl_2$, 1.2 μM ATP, 10 μM DTT, and 25 μM ϵATP in the presence of profilin and/or $GP_5GP_5GP_5$ peptide at various concentrations. Reactions were carried out at 20 °C and initiated with the addition of 95 μM of platelet actin in G-buffer. Profilin (6 μM) was kept in G-buffer, and concentrated trimeric $GP_5GP_5GP_5$ peptide (5 mM) was in 2 mM Tris (pH 7.2). Profilin and the peptide had no effect on the fluorescence of ϵATP.

Infection of Tissue Culture Cells. The PtK2 cell line (derived from the kidney epithelium of the kangaroo rat *Pororous tridactylis*) was seeded at a concentration of 1×10^6 cells per coverslip in 35 mm culture dishes in 3 mL of culture media [MEM with 10% (v/v) fetal calf serum, 1% (w/v) penicillin−streptomycin], and incubated for 72 h at 37 °C and 5% CO_2. The virulent, streptomycin-resistant *L. monocytogenes* strain 10403S (serotype-1) was grown overnight at 30 °C in brain heart infusion (Southwick & Purich, 1994). Bacteria were then washed twice with Hank's balanced salt (Gibco 24020-059) and then resuspended in MEM without antibiotics to give a final concentration of 1×10^7 (or a ratio of 10 bacteria per host cell). Bacteria in 3 mL of culture media were added to each dish followed by centrifugation at 400*g* at room temperature for 10 min and then incubation for 45 min at 37 °C and 5% CO_2. After incubation, extracellular bacteria were removed by washing

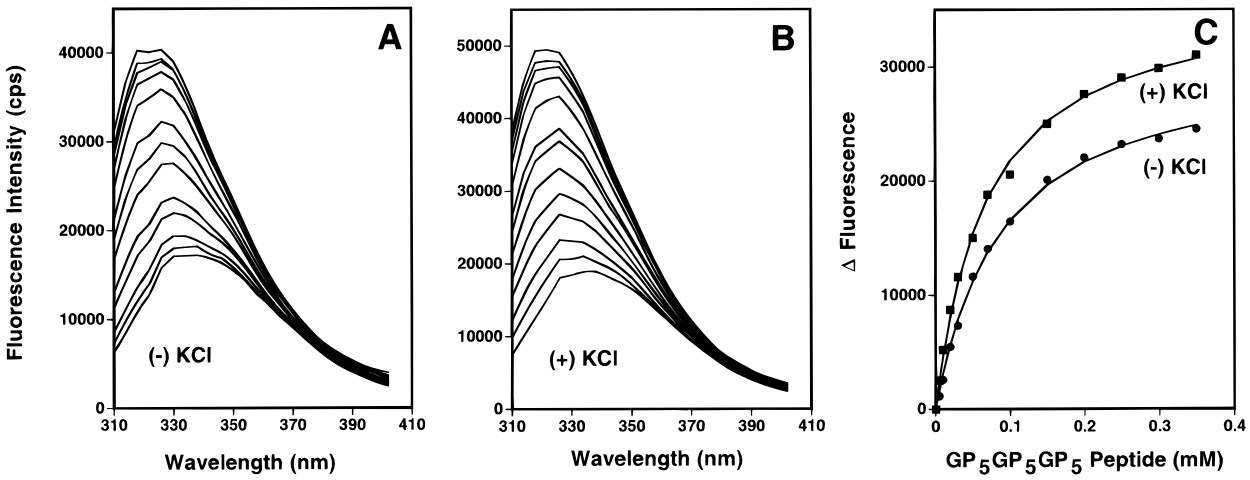

FIGURE 1: Enhancement of intrinsic fluorescence of profilin (5 μM) in the presence of 0 (bottom spectrum), 5, 10, 20, 30, 50, 70, 100, 150, 200, 250, 300, and 350 (top spectrum) μM $GP_5GP_5GP_5$. Samples were prepared by combining stock solutions (containing 20 mM HEPES, 1 mM DTT, pH 7.4) of 5 mM $GP_5GP_5GP_5$ and 44 μM profilin to yield the final concentrations indicated above. (A) Peptide binding in the absence of KCl. (B) Peptide binding in the presence of 150 mM KCl. (C) Plot of the change in intrinsic fluorescence of profilin at 326 nm as a function of $GP_5GP_5GP_5$ concentration. The data points correspond to the experimentally determined fluorescence change, and the solid line is the best fit curve calculated using a quadratic function for a simple dissociation function (i.e., $K_D = ([\text{total profilin}] - x)([\text{total peptide}] - x)/x$, where x is the concentration of profilin−peptide complex).

three times with Hank's balanced salt. The culture media containing gentamicin sulfate (10 μg/mL) was added back to prevent extracellular growth of bacteria. The monolayers were then incubated for 4−6 h, during which time microinjection and video microscopy were performed.

Microscopy and Microinjection. We used a Nikon Diaphot inverted microscope equipped with a cooled charge-coupled device detector (Hamamatsu Instruments, Inc., Tokyo, Japan), and the sample temperature was maintained at 37 °C using a MS-200D bipolar Peltier-cooled perfusion/microincubation system (Narishige Instruments, Tokyo). As previously described (Southwick & Purich, 1994), individual cells were microinjected with peptides using a model 5171 micromanipulator and a model 5242 microinjector (Eppendorf, Inc., Madison, WI). The volume of microinjected peptide corresponded to 8−12% of the total cell volume, and the intracellular concentrations of peptide were taken to be about one-tenth of the needle concentration. Digital images were obtained and processed using an Image-1 computer image analyzer (Universal Imaging, Inc., West Chester, PA). Distances were calibrated using a Nikon micrometer. Velocities of bacterial movement were determined by comparing the images at two time points and measuring the distance traveled by each bacterium using the measure curve length function (Image-I/AT program). Differences in migration velocities were analyzed using the unpaired Student's t test or the Mann−Whitney nonparametric test. For each bacterium, velocity was determined for 3−4 time points before and 6−10 time points after each microinjection. One or several bacteria were analyzed for each microinjected cell. In each experiment, n indicates the number of velocity measurements.

RESULTS

Enhancement of Profilin Fluorescence in the Presence of $GP_5GP_5GP_5$ Peptide. Earlier workers noted that poly-L-proline binds to profilin with a resultant enhancement of the protein's fluorescence emission spectrum (Metzler et al., 1993, 1994; Perelroizen, 1994). They suggested that a minimum stretch of 6−8 prolyl residues may be necessary for binding, and we wanted to determine how well $GP_5GP_5GP_5$, with its stretches of five prolines punctuated by an intervening glycyl residue, binds to profilin. As shown in Figure 1A, the fluorescence emission spectrum of profilin (excitation wavelength = 295 nm) is significantly enhanced in the presence of $GP_5GP_5GP_5$. (There is also a small, but reproducible, shift of the emission spectrum toward the ultraviolet as the concentration of $GP_5GP_5GP_5$ peptide is increased.) Given the likely hydrophobic nature of $GP_5GP_5GP_5$ interactions with profilin, we repeated our binding measurements in the presence of 0.15 M potassium chloride with the expectation that hydrophobic interactions with profilin should be enhanced in the presence of the added electrolyte. As shown in Figure 1B, the observed fluorescence enhancement occurred at slightly lower peptide concentrations in the presence of the added salt, but the effect was not dramatic.

Plotting the observed incremental changes in fluorescence intensity allowed us to quantify the binding behavior, and we obtained a hyperbolic curve for $GP_5GP_5GP_5$ peptide (Figure 1C). Least-squares fitting permitted us to estimate a value of 84 μM for the dissociation constant. The agreement of the experimental data with the theory line calculated for one-to-one complexation of peptide and profilin indicates that a hyperbolic binding isotherm satisfactorily fits the data. We likewise obtained a value of 65 μM for the dissociation constant in the presence of salt. If each GPPPPP constitutes an independent binding site, then the corresponding values for the above dissociation constants must be three times greater.

Effect of $GP_5GP_5GP_5$ on the Exchange Kinetics of Actin-Bound Nucleotide in the Absence and Presence of Profilin. In efforts to understand how the GPPPPP registers help the bacteria to achieve motility, we considered the possibility that profilin's nucleotide-exchange activity may provide some information. While monomeric ATP−actin readily undergoes nucleation and elongation to form actin polymers, ADP−actin appears to be less efficient in the polymerization process. Although actin reversibly binds either ATP or ADP, the spontaneous exchange of bound ATP or ADP with

nucleotide added to the medium is slow. In the presence of profilin, however, actin-bound nucleotide undergoes more rapid exchange with added ATP or ADP. This exchange-facilitating property of profilin may be significant in actin-based motility, especially if actin−ADP is present as a result of net depolymerization at the minus-ends of F-actin or even if actin−ADP is produced during assembly/disassembly cycles at the interface of the bacterial surface and the plus-ends of actin filaments.

For these reasons, we decided to determine whether the GPPPPP sites on VASP can influence the ability of profilin to catalyze this exchange reaction. To monitor the nucleotide exchange reactions in these kinetic experiments (Goldschmidt-Clermont et al., 1991), we employed 1,N^6-etheno-ATP (abbreviated ϵATP), a well-characterized fluorescent analogue of ATP. Actin-bound ϵATP has a substantially greater fluorescence than the uncomplexed fluorophore. All exchange reactions are first-order processes (Frost & Pearson, 1961; Purich & Allison, 1980), allowing use of all fluorescence data obtained over the course of exchange to obtain the exchange rate. Accordingly, we used the following expression for the exchange rate R (in units of M/s):

$$R = -[\mathrm{ATP}][\epsilon\mathrm{ATP}]\{\ln(1 - F)\}/t([\mathrm{ATP}] + [\epsilon\mathrm{ATP}]) \quad (1)$$

where the bracketed species are molar concentrations of ATP and ϵATP, F is the fractional attainment of equilibrium (equal to the reactant concentration at time t divided by its concentration at equilibrium), and t is the time elapsed between initiating and measuring each incremental change during the exchange process.

As shown in Figure 2, recombinant human profilin increases the rate of exchange of actin-bound nucleotide, a finding that is fully consistent with the earlier work of Goldschmidt-Clermont et al. (1991) on actin nucleotide exchange in the presence of this actin-regulatory protein. The half-life for exchange in the absence of added profilin was about 50−60 s, and the half-life was 3−5 s in the presence of 0.1−0.2 μM profilin. For our subsequent experiments, we chose to work at a 20-to-1 molar excess of actin over profilin, and we varied the $GP_5GP_5GP_5$ peptide concentration over the range from 0 to 240 μM. The time courses (shown in Figure 3AB) indicate that the $GP_5GP_5GP_5$ peptide weakly inhibits the rate of nucleotide exchange. Figure 3C is a plot of the net rate of profilin-stimulated exchange (i.e., the rate of exchange in the presence of profilin minus the corresponding rate in the absence of profilin) as a function of $GP_5GP_5GP_5$ peptide concentration. We consistently observed that the $GP_5GP_5GP_5$ peptide has a small, but reproducible, inhibitory effect on the exchange process, whether it is measured in the absence or presence of profilin.

Inhibition of Intracellular Listeria Locomotion by the $GP_5GP_5GP_5$ Octadecapeptide. *Listeria* is thought to achieve intracellular actin-based motility by binding the actin regulatory protein VASP which then utilizes its numerous oligoproline sequences to concentrate profilin molecules onto the bacterial surface. This suggested that shorter peptides, corresponding to the GPPPPP sequence, might competitively block VASP binding to profilin and thereby inhibit bacterial locomotion. Intracellular microinjection experiments do suffer several inherent limitations (e.g., difficulties in attaining uniform delivery of a fixed volume of peptide, variability in cell size and volume, as well as some sensitivity

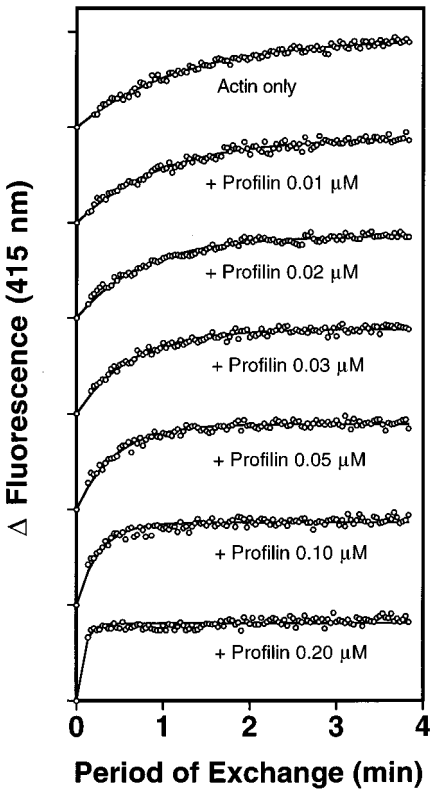

FIGURE 2: Effect of profilin on the time course of the exchange of ϵATP for ATP bound to G-actin. For all cases, the symbols represent the experimental values of fluorescence intensity at different time points. Because the concentrations of exchange reactants were the same in these measurements, the magnitude of maximum change of the fluorescence also remained the same in all cases. The solid lines are time courses generated by fitting the experimental data using the equation described in the text. The determined first-order rate constants are 0.013, 0.017, 0.022, 0.027, 0.038, 0.064, and 0.20 s^{-1} for 0.6 μM actin in the presence of 0, 0.01, 0.02, 0.03, 0.05, 0.10, and 0.20 μM profilin, respectively.

to the distance from site of injection to site(s) of migrating bacteria). Nonetheless, the method does provide valuable semiquantitative data on the behavior of peptide inhibitors within cells.

When the $GP_5GP_5GP_5$ peptide was microinjected (needle concentration = 100−120 μM) into *Listeria*-infected PtK2 cells, the resulting intracellular concentration of 10−12 μM led to rapid cessation of *Listeria* movement (see micrographs presented as Figure 4A−D). Figure 4E shows a typical plot of the rates of *Listeria* motility before and immediately following microinjection of this peptide (intracellular concentration $\approx$ 10 μM). In time-lapse video observations of over fifty bacteria in different infected PtK2 cells, we consistently found that 10 μM $GP_5GP_5GP_5$ immediately stopped the *Listeria* locomotion. Lower intracellular concentrations $GP_5GP_5GP_5$ (5 μM and below) were less effective in the inhibition of motility, and occasionally motility was only temporarily slowed (data not shown).

Although the observed inhibition by the $GP_5GP_5GP_5$ peptide is consistent with the idea that profilin plays a role in promoting the growth of the rocket tails, we conducted two additional sets of microinjection experiments. First, we determined that similar intracellular concentrations of poly-L-proline (10 μM) failed to inhibit *Listeria* motility (see Table 1), indicating that the periodic presence of the glycine residue in the peptide may alter the nature of profilin interactions with proline-rich sequences. And second, we microinjected

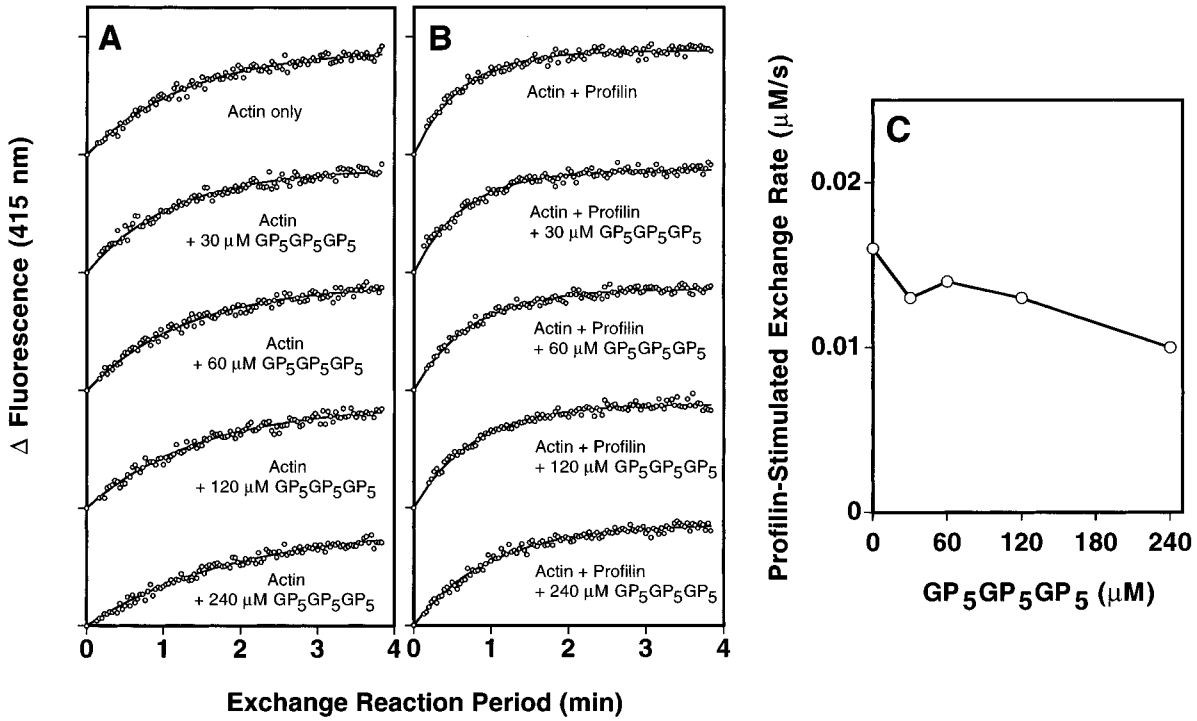

FIGURE 3: Time course of the exchange of ϵATP for ATP bound to G-actin. (A) Effect of $GP_5GP_5GP_5$ peptide alone. (B) Effect of $GP_5GP_5GP_5$ peptide plus profilin. For all cases, the symbols represent the experimental values of fluorescence intensity at different time points. The solid lines are progress curves generated by fitting the experimental data using the equation described in the text. The determined first-order rate constants are 0.013, 0.015, 0.013, 0.011, and 0.009 s^{-1} for 0.6 μM actin in the presence of 0, 30, 60, 120, and 240 μM $GP_5GP_5GP_5$ peptide, respectively, and 0.027, 0.025, 0.022, 0.021, and 0.017 s^{-1} for 0.6 μM actin plus 0.03 μM profilin in the presence of 0, 30, 60, 120, and 240 μM $GP_5GP_5GP_5$ peptide, respectively. (C) Effect of $GP_5GP_5GP_5$ peptide on net rate of profilin-stimulated exchange of ϵATP for actin-bound ATP. The symbols represent the exchange rates derived from the rate constants shown in panels A and B.

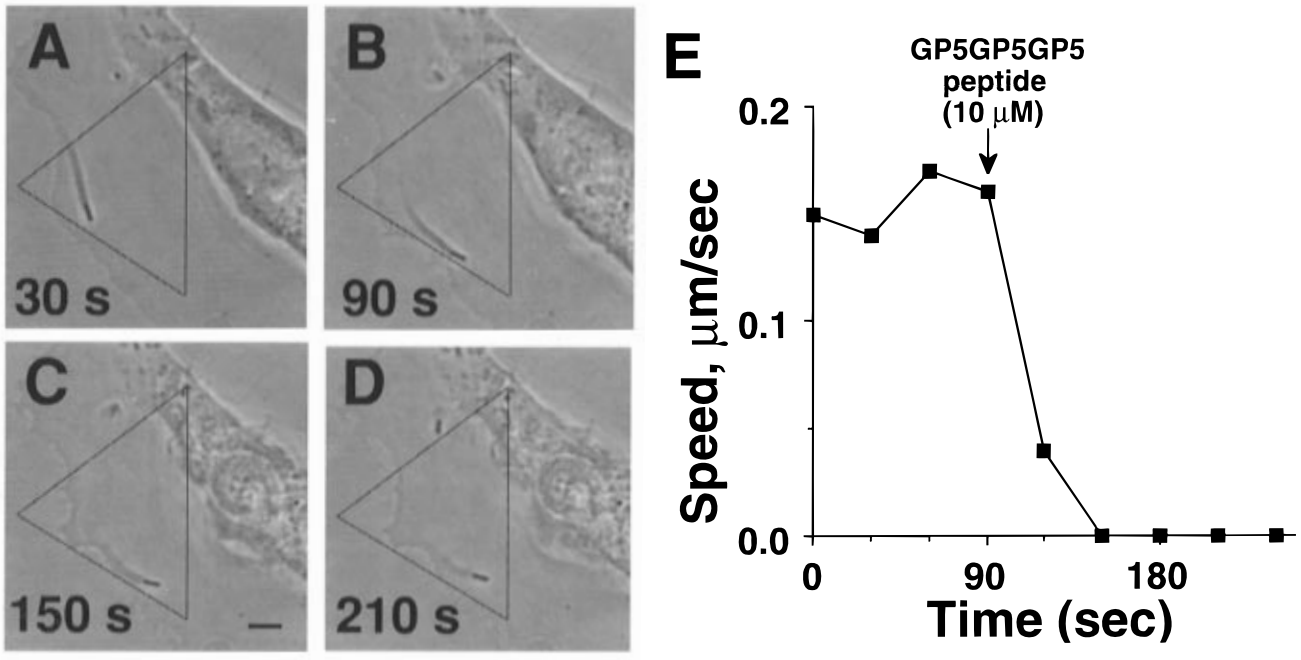

FIGURE 4: (A−D) *Listeria* motility in infected PtK2 cells before and after microinjection of the $GP_5GP_5GP_5$ peptide. Note that all bacterial movement is arrested after microinjection with 10−12 μM $GP_5GP_5GP_5$ peptide. (E) Rate of *Listeria* motility in infected PtK2 cells before and after microinjection of the $GP_5GP_5GP_5$ peptide (approximate intracellular concentration = 10 μM). The vertical arrow indicates the time of microinjection.

equimolar solutions of the $GP_5GP_5GP_5$ peptide and profilin (intracellular concentration = 10 μM of each). We reasoned that the presence of added profilin should neutralize the inhibitory action of the peptide. These microinjection experiments are summarized in Table 1 which gives the pre- and postinjection speeds of bacterial motility, as well as the ratio of their values. The data confirm that microinjection of profilin alone retards motility, whereas microinjection of an equimolar concentration of $GP_5GP_5GP_5$ and profilin neutralizes the peptide's inhibitory effects. While these techniques are not quantitative, coinjection consistently stimulated the actin-based motility of the bacteria (i.e., compare the ratios of the post- to preinjection velocities shown in the fourth column). Note that microinjection of

Table 1: Rate of *Listeria* Motility before and after Microinjecting Oligoproline Peptides in the Absence or Presence of Wild-Type Profilin

additions (concn)	$V_{preinjection}$ (mean μm/s, SD)	$V_{postinjection}$ (mean μm/s, SD)	V_{post}/V_{pre}	*P* value
$GP_5GP_5GP_5$ (5 μM)	0.09 ± 0.04 (n = 48)	0.06 ± 0.09 (n = 48)	0.7	0.001
$GP_5GP_5GP_5$ (10 μM)	0.08 ± 0.04 (n = 27)	0.00 ± 0.01 (n = 27)	0.0	<0.001
poly-L-proline (10 μM)	0.08 ± 0.03 (n = 34)	0.08 ± 0.03 (n = 54)	1.0	NS[a]
profilin (10 μM)	0.08 ± 0.04 (n = 25)	0.04 ± 0.08 (n = 40)	0.5	<0.001
$GP_5GP_5GP_5$ + profilin (10 μM) (10 μM)	0.08 ± 0.04 (n = 31)	0.14 ± 0.06 (n = 70)	1.75	0.001
poly-L-proline + profilin (10 μM) (10 μM)	0.10 ± 0.04 (n = 34)	0.10 ± 0.06 (n = 32)	1.0	NS

[a] NS, not statistically significant.

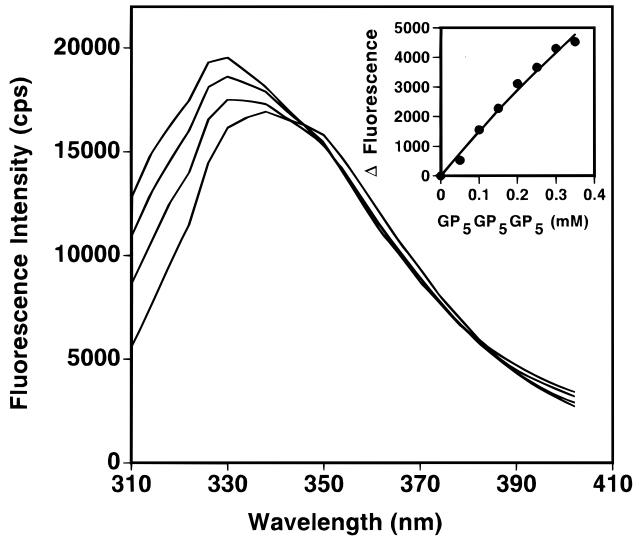

FIGURE 5: Fluorescence emission spectra of the [His-133-Ser]-profilin mutant in the absence (bottom spectrum) and presence of 0.1, 0.2, and 0.3 mM (top spectrum) $GP_5GP_5GP_5$ peptide. Inset: Plot of the change in fluorescence of [His-133-Ser]-profilin at 326 nm as a function of $GP_5GP_5GP_5$ concentration. The data points correspond to the experimentally determined fluorescence change, and the solid line is the best fit curve calculated using the same method described in Figure 1.

poly-L-proline in the absence or presence of profilin had no effect on intracellular locomotion of *Listeria*, suggesting that the $GP_5GP_5GP_5$ and poly-L-proline have distinctly different modes of action within the cell.

Interactions of the $GP_5GP_5GP_5$ Triple Repeat Peptide with [His-133-Ser]-Profilin. The ability of profilin to relieve the inhibitory effects of $GP_5GP_5GP_5$ peptide can be explained by the formation of profilin−$GP_5GP_5GP_5$ complex. Nonetheless, we sought an additional independent test of this mechanism by using a form of profilin unable to interact with the oligoproline sequence. Bjorkegren et al. (1993) recently reported that the His-133-Ser point mutant of profilin fails to bind poly-L-proline, and we confirmed that the same was true for $GP_5GP_5GP_5$ peptide, based on fluorescence titration experiments. As shown in Figure 5, we observed that the $GP_5GP_5GP_5$ peptide induced only a minor enhancement (i.e., an increase that was about 5−6 times smaller than that shown in Figure 1.). The inset to Figure 5 is a plot of the incremental change of fluorescence versus peptide concentration, and the data give no indication of saturation binding behavior. At best, the dissociation constant for $GP_5GP_5GP_5$ complexation with [His-133-Ser]-profilin must be greater than 2−3 mM or at least 30 times weaker than that observed with wild-type profilin.

The very weak binding of the GPPPPP analogue to mutant profilin should be likewise reflected in the inability of this mutant to neutralize the inhibitory effect of $GP_5GP_5GP_5$ on intracellular *Listeria* motility. Indeed, co-injection of this mutant along with the $GP_5GP_5GP_5$ peptide failed to reverse or even partially relieve the peptide's inhibitory effects on *Listeria* motility (see Table 2), even when the [His-133-Ser]-profilin was added in a three-times molar excess over the concentration of $GP_5GP_5GP_5$ peptide. When we microinjected the His-133-Ser point profilin mutant alone into *Listeria*-infected PtK-2 cells, we also found that an intracellular concentration of 10 μM mutant profilin had no discernible effect on the locomotory properties of the microbial pathogen. Together the observations presented in Tables 1 and 2 indicate that the $GP_5GP_5GP_5$ peptide blocks the accumulation of profilin onto the surface of motile *Listeria*, thereby arresting intracellular motility of the pathogen.

DISCUSSION

Mounting evidence points to the central importance of oligoproline sequences as docking sites for actin-regulatory proteins directly involved in actin-based motility (Southwick & Purich, 1996; Zeile et al., 1996). The ABM-1 class of oligoproline sequences is exemplified by the FEFPPPPTDE-type sequences found in *Listeria* ActA surface protein (Purich & Southwick, 1997). These ABM-1 sequences attract the vasodilator-stimulated phosphoprotein VASP to the bacterial surface (Chakraborty et al., 1995). VASP is a tetramer, and each subunit has a contiguous GPPPPPGPPPPPGPPPPP triple-repeat sequence (or $GP_5GP_5GP_5$) as well as single GPPPPP and GPPAPP stretches. These oligoproline sequences, now termed ABM-2 sequences (Purich & Southwick, 1997), were hypothesized to bind profilin. This versatile regulatory protein can function (a) by sequestering monomeric actin, (b) by capping the barbed ends of actin filaments, and (c) by facilitating exchange of actin-bound nucleotide. Our studies confirm that this binding interaction occurs in vitro as well as within the cell. Other experiments addressed the nature of profilin binding interactions with the $GP_5GP_5GP_5$, thus providing additional clues about the action of regulatory protein in promoting bacterial locomotion.

We have determined that microinjection of the $GP_5GP_5GP_5$ peptide blocks intracellular locomotion of *Listeria*. Maximal inhibition is observed after 30−90 s, and the

Table 2: Rate of *Listeria* Motility before and after Microinjecting [His-133-Ser]-Profilin in the Absence and Presence of $GP_5GP_5GP_5$ Peptide

additions (concn)	$V_{preinjection}$ (mean μm/s, SD)	$V_{postinjection}$ (mean μm/s, SD)	V_{post}/V_{pre}	*P* value
H133S-profilin (10 μM)	0.09 ± 0.04 (n = 50)	0.10 ± 0.04 (n = 54)	1.11	NS[a]
H133S-profilin + $GP_5GP_5GP_5$ (10 μM) (10 μM)	0.05 ± 0.03 (n = 13)	0.00 ± 0.00 (n = 18)	0	<0.001
H133S-profilin + $GP_5GP_5GP_5$ (30 μM) (10 μM)	0.08 ± 0.02 (n = 6)	0.01 ± 0.03 (n = 5)	0.13	0.03

[a] NS, not statistically significant.

concentration of synthetic peptide required for inhibition corresponds to the profilin concentration (i.e., 5−60 μM) in most non-muscle cells. The inhibitory action of the $GP_5GP_5GP_5$ peptide contrasts with inhibitory properties of synthetic ActA peptide CFEFPPPPTDE (Southwick & Purich, 1994). Microinjection of the latter results in the virtually instantaneous arrest of *Listeria* motility observed, even at submicromolar concentrations (i.e., 50−200 nM). The peptide acts by dispersing VASP from its docking sites on the surface of motile *Listeria* (Chakraborty et al., 1995). Of course, intracellular experiments are never as straightforward as biochemical investigations, and there may be other oligoproline sequences involved in regulating signal transduction and cellular metabolism. In the case of the GPPPPP triple repeat peptide, inhibition is completely reversed by the addition of an equimolar concentration of profilin; however, no reversal occurs with an equivalent concentration of a mutant profilin that cannot bind to either poly-L-proline or the $GP_5GP_5GP_5$ peptide analogue.

Metzler et al. (1993, 1994) and Perelroizen et al. (1994) suggested that profilin probably requires six or more prolyl residues within a synthetic homopolymer to achieve binding. Details of binding affinity, stoichiometry, as well as definition of subsite recognition can be blurred with unnatural homopolymers. Recent investigations indicated that the vasodilator-stimulated phosphoprotein VASP has multiple GPPPPP sequence repeats for profilin binding, raising the idea that flanking α-amino acid residues might influence the nature of profilin binding. While profilin exhibits a slightly higher affinity for poly-L-proline compared to the $GP_5GP_5GP_5$, both display roughly the same affinities when corrected for the number of prolyl residues per peptide chain. Without cues to indicate the binding register, however, homopolymers are likely to engage in nonspecific interactions that limit the stoichiometry of profilin binding. Although clearly beyond the scope of the present study, future experiments with $GP_nGP_nGP_n$ peptides (where n = 3, 4, 5, 6) and $XP_5XP_5XP_5$ peptides (where X is gly, ala, or pro) may yield additional insight about the nature of the GP_5 binding interaction with profilin. In addition to its single GPPPPP stretch and the $GP_5GP_5GP_5$ triple repeat, VASP also contains GPPAPP and GPPPAPP sequences. If these sequences also bind profilin, the VASP tetramer contains up to 24 potential profilin binding sites.

To our knowledge, the special properties of clustered binding sites have not been previously considered in terms of facilitating actin polymerization. The ActA protein contains a membrane-spanning region that ensures its firm anchoring to the bacterial surface; in the presence of intracellular stores of VASP, this creates an activated cluster on the bacterial surface (see Figure 6). Such a cluster constitutes a discrete subcellular compartment. A nominal

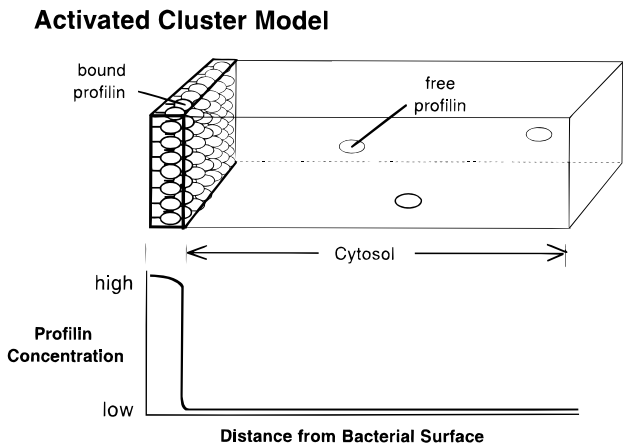

FIGURE 6: Activated cluster model for localizing profilin on the tip of a locomoting *Listeria* bacterium. An open-sided compartment with a volume of 10^{-17} L containing 90−100 ActA molecules can bind up to 360−400 VASP tetramers and create an effective molarity of 1.4−1.6 mM GPPPPP sites for binding profilin. The compartment's dimensions correspond to a 0.5 μm × 0.5 μm patch on the bacterium's tip and a depth of 30 nm corresponding to the nominal outward reach of the ActA polypeptide from the bacterial surface. The accompanying plot illustrates how the concentration gradient would abruptly drop off as the distance from the membrane surface exceeds the outward reach of the tethered VASP molecules.

layer of 20−30 nm (i.e., the outward reach of membrane-bound protein) creates a 10^{-17} L volume (i.e., 0.5 μm × 0.5 μm × 0.03 μm) at the tip of a bacterium; this requires only 40−50 tethered ActA molecules which use their four FEFPPPPTDE repeats to attract 160−200 molecules of the vasodilator-stimulated phosphoprotein VASP. Each VASP molecule has 24 oligoproline sequences, allowing a surface patch to attain effective concentration of 0.8−1.2 mM binding sites for profilin. This is well above the K_D for profilin binding to GPPPPP registers. Moreover, this number of ActA molecules would amount to only 2−3% of the total membrane protein present in a gram-positive bacterium like *Listeria*, suggesting that our estimates are well within reason. A fascinating feature is the absence of any concentration gradient (i.e., the system has two phases composed of a densely concentrated layer at the tip of the bacterium and a low-concentration cytosolic phase). This may help to localize profilin and/or profilin−actin−ATP and promote nucleation, a process that is much more favorable at high actin−ATP concentrations. A second special property is that the concentration of profilin and/or profilin−actin−ATP within such a small volume element cannot remain steady; indeed, chemical systems always exhibit fluctuations or excursions from the average concentration (Magde, 1977). The thin layer or film created by tethered ActA molecules at the trailing end of a locomoting *Listeria* may allow local concentrations of actin−ATP to fluctuate above the concentration needed for efficient nucleation. Finally, a third

property is that movement of this densely concentrated binding layer through the cytoplasm during actin-based bacterial motility permits the bacterium to replenish constantly its supply of profilin and/or profilin−actin−ATP as the bacterium moves within the peripheral cytoplasm. In any event, one or several of these properties, each arising from high-density clustering, may create the activated membrane complex required for actin-based *Listeria* motility.

The observed K_D of 84 μM for $GP_5GP_5GP_5$ peptide complexation with profilin indicates that binding interaction is relatively weak. Nevertheless, indirect immunofluorescence microscopy has already demonstrated that profilin is localized at the trailing end of migrating *Listeria*, precisely at the bacteria/rocket-tail interface (Chakraborty et al, 1995; Pistor et al., 1995). Furthermore, our microinjection experiments indicate that the synthetic peptide is a much better ligand for profilin within cells, and other factors present within cells may reduce the K_D for $GP_5GP_5GP_5$ peptide. Alternatively, the peptide may selectively interact with a pool of profilin, perhaps profilin−actin−ATP, thereby blocking its accumulation on the tip of motile bacteria. We should also note that weak binding of profilin to VASP's GPPPPP registers probably permits rapid replacement of profilin by profilin−actin−ATP. Because much of profilin is complexed with actin−ATP, future work must address the nature of the competition of profilin and profilin−actin−ATP for VASP.

$GP_5GP_5GP_5$ peptide weakly inhibited exchange of actin-bound nucleotide in the absence or presence of profilin. While we had anticipated that binding of profilin to the VASP peptide might increase nucleotide exchange, there are several mechanisms that would allow loosely bound profilin to promote rocket tail assembly. In the first case, low-affinity complexation of profilin with the GP_5 repeats would establish an equilibrium between pools of tethered and free profilin. In a sense, bound profilin may act to buffer the local free profilin concentration at the interface of the bacterium and rocket tail. This could sustain bacterial motility whenever the immediate supply of profilin within the cytoplasm falls below a threshold concentration needed for motility. As noted above, low-affinity binding also suggests that the rate of profilin dissociation from VASP should be fast, thereby permitting rapid release of free profilin that could promote nucleotide exchange. Such behavior would be unaffected by the inhibition of profilin-mediated nucleotide exchange by $GP_5GP_5GP_5$. Alternatively, VASP's $GP_5GP_5GP_5$ registers may facilitate local release of actin−ATP from profilin−actin−ATP complex at the junction of the bacterial surface and the growing rocket tail. The critical concentration for actin−ATP binding to the barbed ends of actin filaments is about 0.1−0.2 μM; however, the concentration profilin−actin complex is thought to be significant in nonmuscle cells, and the high intracellular [ATP]/[ADP] ratio favors formation of profilin−actin−ATP complex. Any facilitated dissociation of profilin−actin−ATP complex would directly increase supply actin−ATP to growing filaments.

Contrary to the conclusions of Tilney and Portnoy (1989) and Tilney et al. (1992a,b) regarding rocket tail filament organization, Sechi et al. (1997) very recently demonstrated convincingly that the major component of the *Listeria* rocket tail is composed of long actin filaments. These investigators offered an attractive model that explained the length and orientation of longitudinal and transverse actin filaments within bacterial filopods in terms of a polymerization zone on the bacterial surface. This zone accelerates filament assembly without increasing the spontaneous nucleation and capture of new filaments, and the zone may also suppress filament capping. Our cluster model for activating actin-based motility fits nicely with their ideas concerning an active polymerization zone.

Symons et al. (1996) suggested that Wiskott−Aldrich syndome protein (or WASP) also contains proline-rich sequences that are structurally related to VASP. WASP is an effector of cdc42, a protein that regulates cell polarity, and mutations in WASP result in Wiskott−Aldrich syndome, a disorder characterized by thrombocytopenia, recurrent infections, defective T and B cell function, and eczema (Symons et al., 1996). Both VASP and WASP share several homologous motifs, including ABM-2 stretches suitable for binding of profilin (Purich & Southwick, 1997). Their distinctive tissue distributions may allow them to differentially modulate actin polymerization in various nonmuscle cell types. Other proline-rich actin cytoskeletal proteins include (a) verprolin, a regulatory protein which plays a role in cytoskeletal organization in *Saccaromyces cerevisiae* (Donnelly, et al., 1993); (b) Ena, the protein product expressed by the *Drosophila* gene *Enabled* (Gertler et al., 1995); and (c) zyxin, a focal contact protein (Sadler et al., 1992). These proteins also frequently contain oligoproline sequences with five or more proline residues preceded by a glycyl or alanyl residue. Thus, by selectively expressing one or more of these cytoskeletal regulatory proteins, a particular nonmuscle cell may achieve a spectrum of options for engaging profilin in the dynamic reorganization of the actin cytoskeleton.

Finally, because microbial pathogens employ molecular mimicry to usurp and/or defeat host cell processes, principles of *Listeria* locomotion are also apt to apply to actin-based motility in uninfected host cells. Presumably, there are host cell analogues, acting much as the *Listeria* ActA surface protein, that serve as a key elements within a cascade of binding reactions designed to concentrate profilin and to stimulate actin filament assembly. Recent studies suggest that the focal adhesion components zyxin (Rheinhard et al., 1995) and vinculin (Southwick et al., 1996) bind to VASP, and these proteins may stimulate profilin's promotion of actin-based locomotory processes.

REFERENCES

Bjorkegren, C., Rozycki, M., Schutt, C. E., Lindberg, U., & Karlsson, R. (1993) *FEBS Lett. 333*, 123−126.

Chakraborty, T., Ebel, F., Domann, E., Pistor, S., Temm-Grove, C. J., Jockusch, B. M., Reinhard, M, Walter, U., & Wehland, J. A. (1995) *EMBO J. 14*, 1314−1321.

Dabiri, G. A., Sanger, J. M., Portnoy, D. A., & Southwick, F. S., (1990) *Proc. Natl. Acad. Sci. U.S.A. 87*, 6068−6072.

Donnelly, S. F., Pocklington, M. J., Pallota, D., & Orr, E. (1993) *Mol. Microbiol. 10*, 585−596.

Fedorov, A. A., Pollard, T. D., & Almo, S. (1994) *J. Mol. Biol. 241*, 480−482.

Frost, A. A., & Pearson, R. G. (1961) *Kinetics and Mechanism*, 2nd ed., Wiley, New York.

Gertler, F. B., Comer, A. R., Juang, J., Ahem, S. M., Clark, M. J., Liebel, E. C., & Hoffmann, M. (1995) *Genes Dev. 9*, 521−533.

Goldschmidt-Clermont, P. J., Machesky, L. M., Doberstein, S. K., & Pollard, T. D. (1991) *J. Cell Biol. 113*, 1081−1089.

Kocks, C., Gouin, E., Tabouret, M., Berche, P., Ohayon, H., & Cossart, P. (1992) *Cell 68*, 521−531.

Machesky, L. M., Cole, N., Moss, B., & Pollard, T. D. (1994) *Biochemistry 33*, 10815−10824.
Magde, D. (1977) in *Chemical Relaxation in Molecular Biology* (Pecht, I., & Rigler, R., Eds.) Molecular Biology, Biochemistry, and Biophysics 24, pp 43−83, Springer-Verlag, Berlin.
Metzler, W. J., Constantine, K. L., Friedrichs, M. S., Bell, A. J., Ernst, E. G., Lavoie, T. B., & Mueller, L. (1993) *Biochemistry 32*, 13818−13829.
Metzler, W. J., Bell, A. J., Ernst, E., Lavoie, T. B., & Mueller, L. (1994) *J. Biol. Chem. 269*, 4620−4625.
Perelroizen, I., Marchand, J.-P., Blandchoin, L., Didry, D., & Carlier, M.-F. (1994) *Biochemistry 33*, 8472−8478.
Pistor, S., Chakraborty, T., Walter, U., & Wehland, J. (1995) *Curr. Biol. 5*, 517−525.
Purich, D. L., & Allison, R. D. (1980) *Methods Enzymol. 64*, 3−46.
Purich, D. L., & Southwick, F. S. (1997) *Biochem. Biophys. Res. Commun. 231*, 686−691.
Reinhard, M., Jouvenal, K., Tripier, D., & Walter, U. (1995) *Proc. Natl. Acad. Sci. U.S.A. 92*, 7956−7960.
Sadler, I., Crawford, A. W., Michelsen, J. W., & Beckerle, M. C. (1992) *J. Cell Biol. 119*, 1573-1587.
Sanger, J. M., Sanger, J. W., & Southwick, F. S. (1992) *Infect. Immun. 60*, 3609−3619.
Sechi, A. S., Wehland, J., & Small, J. V. (1997) *J. Cell. Biol. 137*, 155−167.
Southwick, F. S., & Purich, D. L. (1994) *Proc. Natl. Acad. Sci. U.S.A. 91*, 5168−5172.
Southwick, F. S., & Purich, D. L. (1995) *BioEssays 16*, 885−891.
Southwick, F. S., & Purich, D. L. (1996) *N. E. J. Med. 334*, 770−776.
Southwick, F. S., Laine, R. O., Kang, F., Zeile, W., & Purich, D. L. (1996) *Mol. Cell Biol. 7*, 380a.
Symons, M., Derry, J. M. J., Karlak, B., Jiang, S., Lemahieu, V., McCormick, F., & Francke, U. (1996) *Cell 84*, 723−734.
Tanaka, M., & Shibata, H. (1985) *Eur. J. Biochem. 151*, 291−297.
Theriot, J. A., Mitchison, T. J., Tilney, L. G., & Portnoy, D. A. (1992) *Nature (London) 357*, 257−260.
Tilney, L. G., & Portnoy, D. A. (1989) *J. Cell Biol. 109*, 1597−1608.
Tilney, L. G., DeRosier, D. J., & Tilney, M. S. (1992a) *J. Cell. Biol. 118*, 71−82.
Tilney, L. G., DeRosier, D. J., Weber, A., & Tilney, M. S. (1992b) *J. Cell. Biol. 118*, 83−93.
Tseng, P. C.-H., Runge, M. S., Cooper, J. A., & Pollard, T. D. (1984) *J. Cell Biol. 98*, 214−221.
Way, M., Pope, B., Gooch, J., Hawkins, M., & Weeds, A. G. (1990) *EMBO J. 9*, 4103−4109.
Weber, A., Nachmias, V. T., Pennise, C. R., Pring, M., & Safer, D. (1992) *Biochemistry 31*, 6179−6185.
Zeile, W., Purich, D. L., & Southwick, F. S. (1996) *J. Cell Biol. 133*, 49−59.

BI970065N